24th INTERNATIONAL CONGRESS ON SOUND AND VIBRATION
23–27 July 2017, London

ICSV24
23-27JULY 2017
LONDON CALLING

# MODELLING THE UNSTEADY FLOW AND SHOCK-ASSOCIATED NOISE FROM DUAL-STREAM TURBULENT JETS

Aldo Rona, Alessandro Mancini, and Edward Hall
*University of Leicester, Department of Engineering, LE1 7RH, England, UK*
*email: ar45@le.ac.uk, am791@le.ac.uk, eh171@le.ac.uk*

Sustained demand for more fuel efficient, environmentally friendly, and quieter aircraft power plants is promoting the development of higher bypass engines for large transport aircraft. These turbofan engines feature a fan of larger diameter, providing a larger fraction of the thrust by expansion through the secondary (annular) nozzle. This fixed-geometry nozzle is typically run choked at cruise conditions, generating an under-expanded co-axial jet with a significant broad-band shock-associated noise signature. The three-dimensional shock-shear layer flow dynamics of a dual stream jet was modelled by Detached Eddy Simulations, using a simplified staggered coaxial round dual-nozzle geometry without a central plug. Predictions were obtained using an in-house up to third order space accurate finite-volume scheme based on the Roe approximate Riemann solver, using a tuneable Sweby flux limiter for capturing the unsteady shocks. Flow conditions were taken as representative of secondary nozzle turbofan engine operations in cruise. The primary nozzle was modelled subsonic and cold, to allow comparison with static jet measurements, for validation purposes. Large Eddy Simulations obtained independently using a high-order shock-tolerant code from CERFACS gave further support to the validation and to the flow analysis. The dual-nozzle jet was found to share broad similarities with the more widely studied under-expanded single jet flow, with the interaction between the unsteady outer shear layer and the shock train generating broadband shock-associated noise. The axial stagger between the primary and secondary nozzles was found to have a strong influence on the first shock cell and on the flow downstream of it. Predictions of the radiating pressure field from the dual-stream jet show that the broad-band shock-associated noise component is satisfactorily predicted by Detached Eddy Simulations, by virtue of this contribution occupying a narrower Strouhal number range compared to broad-band turbulence associated nose, for a range of observers located along the jet sideline.

Keywords: Jet noise, Detached Eddy Simulations, Dual-stream jet, Under-expanded jet, Computational aeroacoustics.

## 1. Introduction

Current generation high bypass ratio turbofan engines discharge a dual-stream jet with a high-speed inner jet, from the engine core, and a lower speed coaxial jet, from the fan. Due to the high temperature of the combustion products, the Mach number of the inner jet is typically subsonic, whereas the coaxial jet that delivers most of the engine thrust typically expands from a chocked nozzle. As the coaxial nozzle is convergent and of fixed geometry in current wide-body civil aircraft turbofan engines, shock-free fully expanded jet conditions are achieved only at given aircraft altitude and speed combinations. Air traffic route management constraints require operating the aircraft over a wider flight envelope, with the coaxial jet from the engines under-expanded. This generates shock-associated jet noise (shock-cell noise) radiating towards the cabin.

Shock-cell noise arises from the interaction of convected instabilities in an incorrectly expanded jet shear layer with the shock-cell train [1], resulting in a linear array of sound sources. The constructive interference of the linear array in the upstream direction results in jet screech, a loud form of shock-cell noise [2] that is usually absent in full-scale engine jets but it is often found in laboratory scale model tests. This simple well-established model is used in the current state of art aircraft noise models, such as SOPRANO, developed in FP6 SILENCE(R) and used in FP7 VITAL. A more advanced description of the noise production physics is by the interference of hydrodynamic (shear-layer) waves and upstream-propagating (pressure) waves [3], where the noise generation is by shock-cell leakage in the unsteady flow [4]. In experiment, the innovative use of wavelets [5] and linear stochastic estimation to pressure-decouple the aerodynamic and acoustic fields allows identification of the unsteady flow accelerations responsible for noise generation, therefore guiding noise control concepts by flow control.

Current predictions of jet noise impinging on the fuselage skin of aircraft at cruise rely mostly on data from old flight tests or on mature and legacy empirical models, since accurate predictions using physics-based noise model are very challenging. Low-accuracy cabin noise prediction models drive conservative design choices for cabin acoustic liners, which increases the aircraft weight. This in turns increases the fuel consumption and the environmental impact of aircraft operations.

Underpinning the development of alternative physics-based models for shock-cell noise is the availability of affordable computational fluid dynamic models of the turbofan dual-jet outflow that can resolve, in time, the energy-containing length scales and their compressible interactions that are responsible for the generation of this noise component. Towards this goal, this paper presents a Detached Eddy Simulation (DES) of an idealized dual-flux cold jet and shows that, whereas the DES spatio-temporal resolution of all scales of motion is coarse, it appears that enough time-resolved flow dynamics is captured to reproduce qualitatively the known characteristics of shock-associated noise along the jet sideline.

## 2. Test case conditions

The test case considered in this study is a coaxial jet where the primary flow is cold and subsonic with an exit Mach number of $M_p = 0.89$, a nozzle pressure ratio $CNPR = 1.675$, and the secondary stream is operated at supersonic under-expanded conditions with a design exit Mach number of $M_s = 1.20$ and an annular nozzle pressure ratio $FNPR = 2.45$. The jets are discharged from two concentric convergent nozzles with primary and secondary diameters of $D_p = 23.4mm$ and $D_s = 55.0mm$ respectively. The lip thickness of the two nozzles at the exit is $t = 0.5mm$. The Reynolds numbers based on the jet exit diameters are $Re_p = 0.57 \times 10^6$ and $Re_s = 1.66 \times 10^6$ for the primary jet and the annular jet, respectively.

Experimental and numerical data is available for comparison, provided by the von Karman Institute (VKI) and the Centre Européen de Recherche et de Formation Avancée en Calcul Scientifique (CERFACS) respectively. CERFACS performed a study with matching conditions using the computational fluid dynamics software ***elsA***, developed by ONERA. This is a finite-volume multi-block structured solver with a sixth-order implicit compact finite difference scheme by Lele [6], extended to finite-volumes by Fosso *et al.* [7]. The scheme is stabilized by the compact filter of Visbal & Gaitonde [8] that is also used as an implicit subgrid-scale model for the Large Eddy Simulations (LES). Time integration is performed by a six-step third-order accurate Runge-Kutta Dispersion Relation Preserving (DRP) scheme by Bogey and Bailly [9]. Comparative far-field experimental data was made available by VKI, where tests at similar flow conditions were performed. The comparison of results obtained by the in-house Detached Eddy Simulation software Cosmic with both third party experimental and numerical data is very important to build confidence in the solver capabilities and in its ability to effectively capture the main aeroacoustic phenomena in supersonic free jets.

## 3. Numerical set-up and mesh

Numerical simulations were performed with the in-house code Cosmic, developed at the University of Leicester. Cosmic is a multi-block finite-volume explicit time-resolved Computational Fluid Dynamics (CFD) solver. The code uses a two-dimensional finite-volume four-point stencil approximate Riemann solver by Roe [10] with a Monotone Upstream-centred Scheme for Conservation Laws (MUSCL) interpolation by Van Leer *et al.* [11] to compute the convective fluxes. This gives up to a third-order accurate reconstruction of the spatial gradients in smooth flow regions. In regions of rapidly changing flow, the spatial gradients are limited by the introduction of a Total Variation Diminishing Scheme (TVD) by Sweby [12]. A standard multi-stage second-order Runge-Kutta (RK) integration is used to time-march the flow. The turbulent flux vector is estimated using a second-order accurate gradient reconstruction method, based on the Gauss divergence theorem. The code implements a Detached-Eddy Simulation (DES) approach. The DES approach was developed as an hybrid approach to merge LES and RANS. The reason behind the development of the DES methods is the attempt to reduce the mesh points required for accurately solve the flow close to the wall in three-dimensional simulations. In Cosmic, the RANS closure is provided by means of the $k-\omega$ two-equation model of Wilcox [13], while the LES closure is obtained with the one-equation model of Yoshizawa [14]. The dynamic switching between the RANS and LES methods is performed by a blending function $\Gamma$ [15]. The code has been validated on several academic test cases such as the shock-tube and the spherical expansion as documented in El-Dosoky [16] and has been used to model unsteady cavity flow [17] and transitional boundary layers [18].

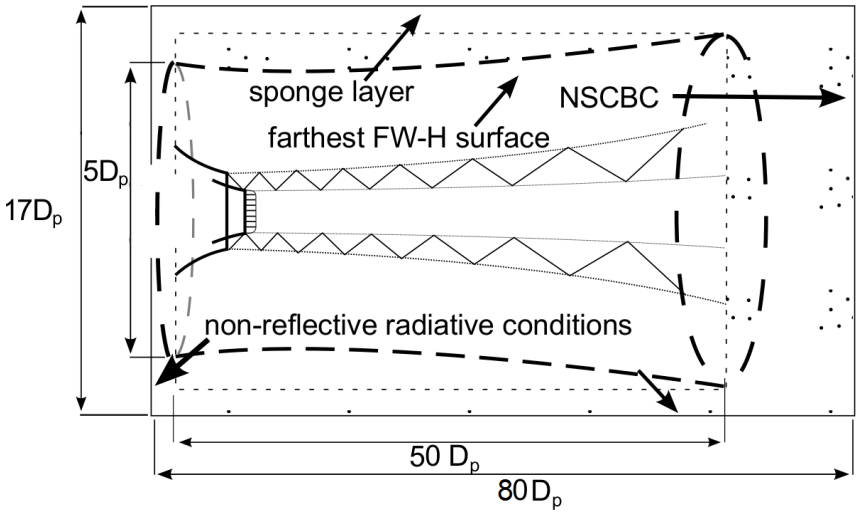


Figure 1: Sketch of the computational domain for the dual jet simulation.

A structured numerical mesh was generated for the numerical solution of the flow governing equations. The mesh for the dual jet has similar features to the single jet mesh used in Pérez-Arroyo *et al.* [19] and a sketch of the domain is shown in Fig. 1. The mesh contains $226 \times 10^6$ cells and is of butterfly type in order to avoid the occurrence of degenerate cell faces at the jet axis. The mesh near the walls of the internal sections of the nozzles, as well as near the external section of the primary nozzle, attain a resolution of $y^+ \approx 1$ at the wall with $25$ points across the boundary layers. The maximum expansion ratio between adjacent cells in the mesh is $\leq 4\%$. The radial domain size grows with the axial position in order to take into account the expansion of the jet, from $r/D_p = 6$ at the exit of the primary nozzle to $r/D_p = 12$ at $x/D_s = 50$.

## 4. Validation

The results obtained with Cosmic for the coaxial jet test case were compared with data from ***elsA***. Time-averaged results are analysed in this section. The averaging process is performed over a period of 120 convective times, calculated as $\tau = t \cdot u_c / D_p$, where $u_c$ is the ambient speed of sound. In Fig. 3, time-averaged Mach iso-contours are shown from Cosmic and ***elsA***. The length of the potential core of the secondary jet differs in the two sets of data. This is expected since Cosmic is based on a low-order scheme and its intrinsic numerical dissipation is higher with respect to that of ***elsA***, resulting in a faster reduction of the flow speed. Figure 4 presents the averaged Mach number distribution along the centreline of the secondary jet. The predicted amplitude of the shock cells is in good agreement between the solvers, however, there is a spatial phase shift in the secondary jet shock train that causes the consequent shift of the structures inside the primary flow.

This phase shift is due to a different flow topology in the region above the primary nozzle wall, where the expansion that develops at the nozzle lip of the secondary nozzle is first reflected as an expansion by the wall itself and then it is reflected as a shock by the shear layer. Figure 2 [20] shows a comparison of the numerical results from ***elsA*** with experimental data provided by VKI. It is possible to observe that, after the first reflected shock (yellow region), there is the formation of a small region of accelerating flow caused by an expansion. This triangular region, which is smaller in the ***elsA*** numerical results compared to experiment, is not visible in the Cosmic results, due to a different interaction of the first shock with the shear layer that develops from the primary nozzle lip. This behaviour is currently under investigation. Despite a poor match for the time-averaged quantities, time-dependent analyses show a good qualitative agreement with ***elsA***, as it is discussed in the next section.

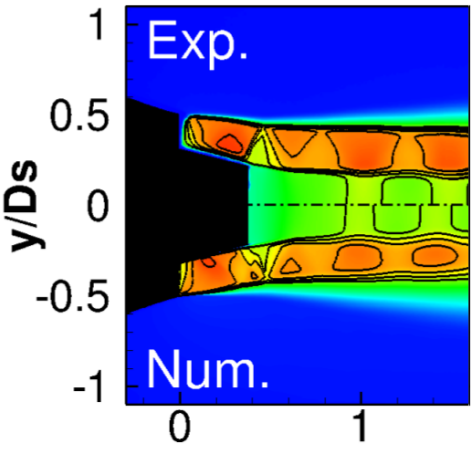


Figure 2: Time-averaged Mach iso-contours. Comparison between LES by ***elsA*** and experiment.

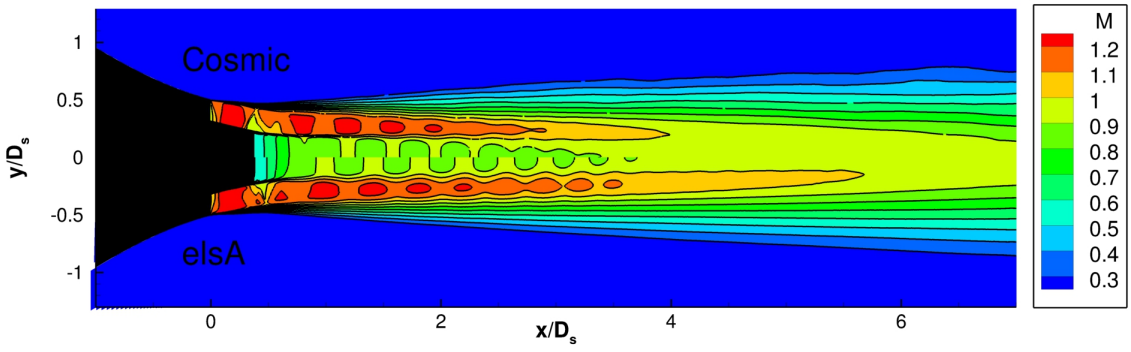


Figure 3: Time-averaged Mach iso-contours. Comparison between Cosmic and ***elsA*** CFD solvers.

## 5. Unsteady flow and noise generation

Figure 5 shows a snapshot taken from the Cosmic DES simulation. Instantaneous Mach number iso-levels are labelled with colours, surrounded by the pressure field fluctuations that are labelled with the grayscale. The key features of a supersonic under-expanded flow can be clearly identified,

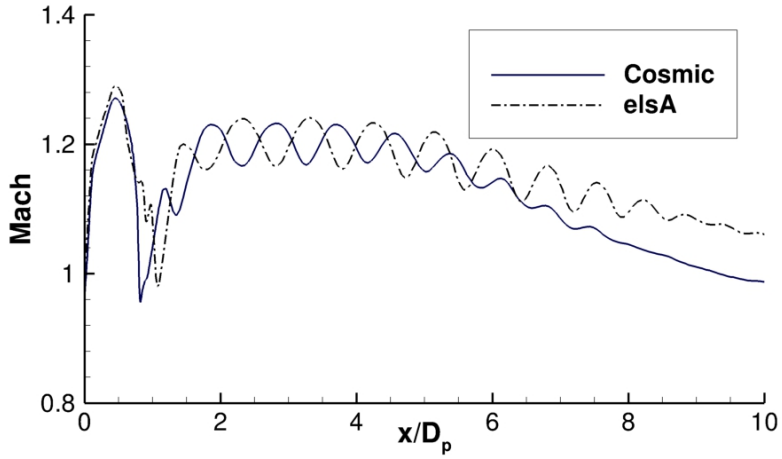


Figure 4: Time-averaged Mach distribution along the centreline of the secondary jet. Comparison between Cosmic and ***elsA*** CFD solvers.

with diamond-shaped shock cells strongly interacting with the turbulence structures being convected downstream inside the mixing layer. Pressure waves are visible and appear to be travelling in both the upstream and downstream directions, indicating that shock-cell noise (SCN) is generated by the jet.

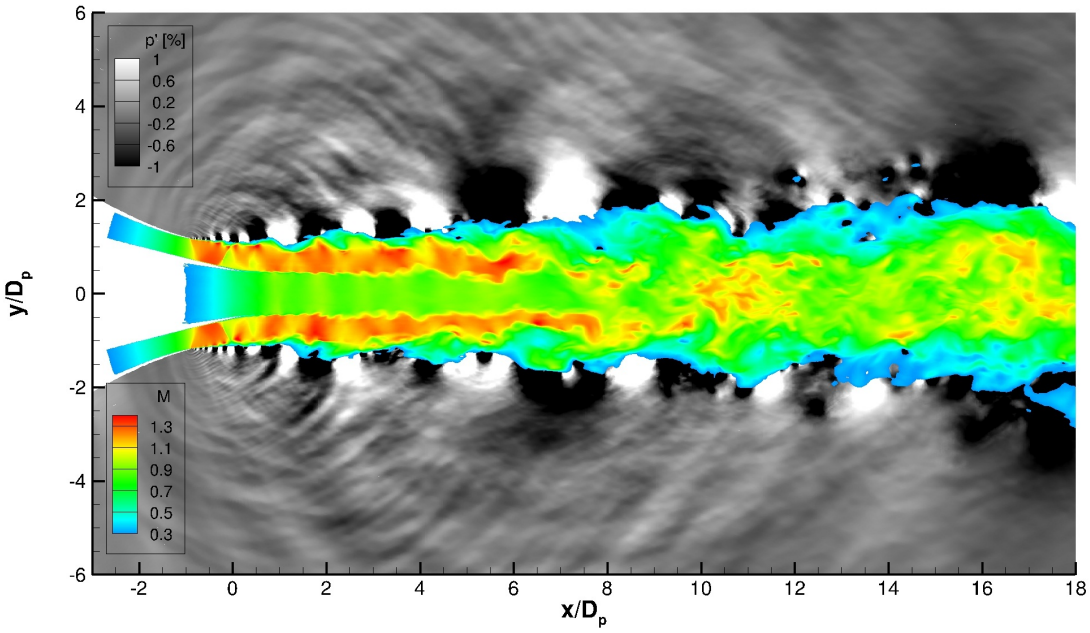


Figure 5: Instantaneous iso-colour levels of streamwise Mach number and grayscale iso-levels of pressure fluctuation.

In Fig. 6, the Power Spectral Density (PSD) in the near field of the jet is shown. Figure 6(a) shows the PSD obtained with ***elsA*** [20] for an array of probes placed at $x = 2D_p$. Figures 6(b) and 6(c) are obtained with Cosmic at $x = 2D_p$ and $x = 3D_p$ respectively. The PSD is expressed in $dB/Hz$ and it is plotted as a function of the axial location and frequency, expressed as a Strouhal number. The probe spacing is equal to $\Delta x = 0.1D_e$. Analysing Fig. 6 with respect to results presented by Savarese [21] for an under-expanded single jet test case, it is possible to observe the 'banana' shaped component of noise at high frequency typical of broad-band shock-associated noise (BBSAN). The extent of the 'banana' is proportional to the shock train structure showing the clear dependence of these frequency components upon the shock cells. The agreement in shape and intensity of the PSD plots is very good

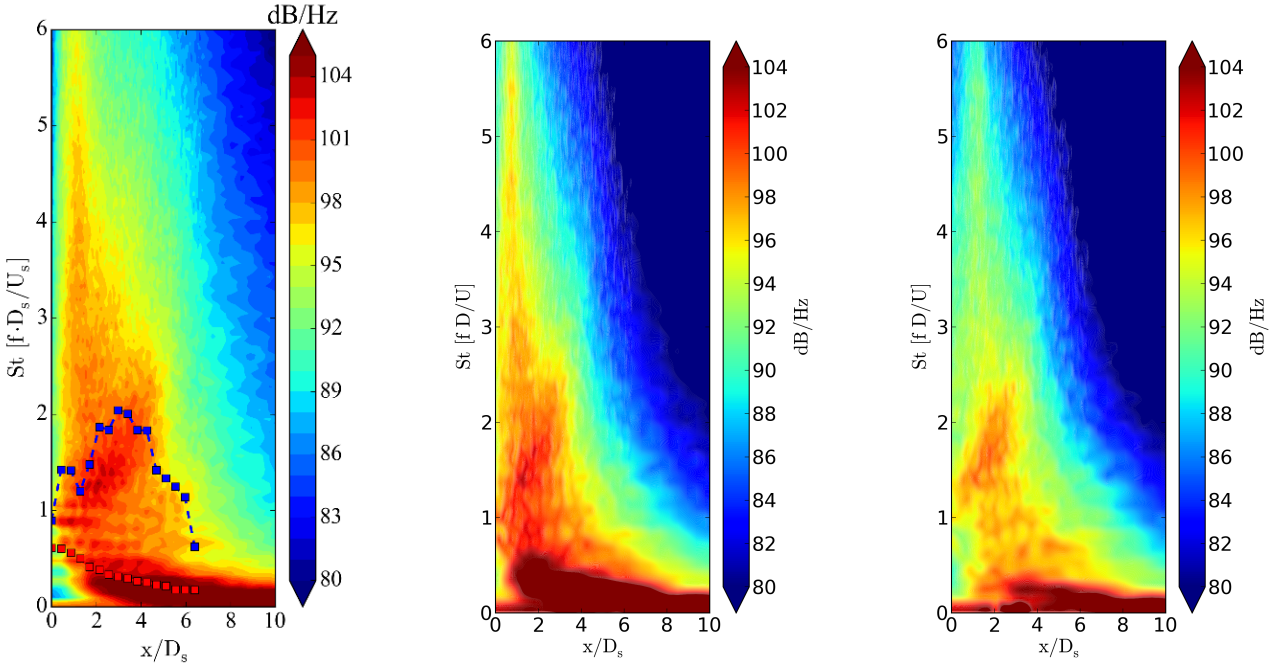


(a) PSD from ***elsA*** [20] at $R = 2D_p$.

(b) PSD from Cosmic at $R = 2D_p$.

(c) PSD from Cosmic at $R = 3D_p$.

Figure 6: Power Spectral Density at different radial locations for a dual jet configuration obtained with Cosmic and ***elsA*** [20] CFD solvers.

and it indicates that the DES simulation is able to correctly capture the fundamental mechanisms of shock-cell noise generation.

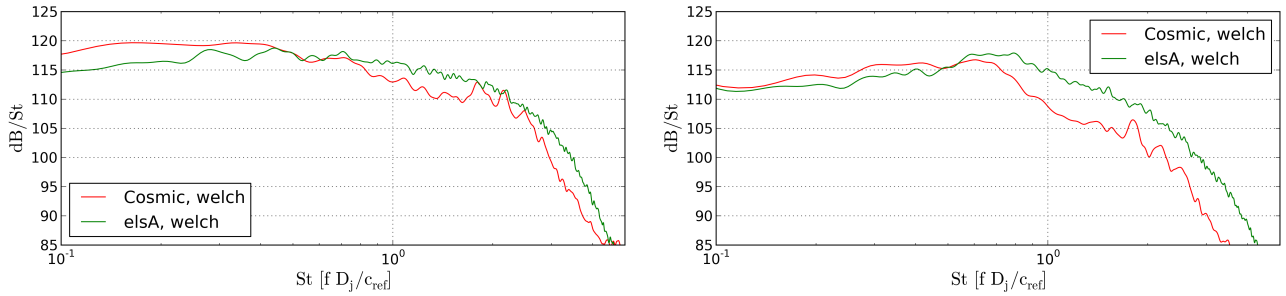


(a) SPL at $50°$.

(b) SPL at $120°$.

Figure 7: Acoustic spectra in the far-field, at $R = 70D_p$. The angle $\theta$ is measured with respect to the jet axis. Numerical results from Cosmic and ***elsA***.

Figure 7 shows Sound Pressure Level (SPL) predictions from far-field probes placed at $R = 70D_p$. These results were obtained by means of the Ffowcs-Williams and Hawkings acoustic analogy applied on surfaces that are conformal to the co-axial jet, as sketched in Figure 1. The predictions of the downstream radiating noise, at $50°$, show a very good agreement over a wide range of frequencies. In the upstream direction, at $120°$, the DES predicts a lower intensity at high frequencies, while the agreement with LES is regained at low frequencies. The overall good agreement indicates that DES are able to provide fairly reliable results both in the near and the far field. This suggests that sufficient time-dependent physics is resolved by DES for predicting the dominant shock-associated aeroacoustic sources in the-coaxial jet.

## 6. Conclusions

This paper provided an insight into the modelling of dual-flux jets performed within the collaborative Marie Curie Integrated Training Network AeroTraNet 2. The Associated Partner Airbus SAS provided a common dual-flux jet configuration and engine operating line as a common target to work towards. A simplified geometry without plug was used to represent the forthcoming generation of turbofan engines for civil transport, featuring an increased by-pass ratio and staggered nozzles. A programme of computationally intensive Large Eddy Simulations (LES) at CERFACS resolved the flow and near-field pressure unsteadiness in great detail. This has generated a database that was used for testing the approximation level of less computationally expensive methods. This result was achieved through concurrent significant advances in the LES code, by implementing shock-tolerant algorithms compatible with the high-order solver [22]. An important contribution came from the interaction between the French and the UK researchers, enabled by AeroTraNet 2. The less computationally demanding Detached Eddy Simulation, using a lower-order solver, was found to be able to reproduce enough of the flow dynamics to deliver, within limits, the characteristic radiating near-field component of broad-band shock-associated noise, as noted in Fig. 6. The timescales of this computationally lighter method, being of the order of one week on current high performance computing clusters, are sufficient for considering this tool in the design timescale of manufacturers of airframes and of aircraft engines.

## 7. Acknowledgements

The dissemination of these results has received funding from the European Union Seventh Framework Programme FP7/2007-2013 under grant agreement no. 317142. The advice received at the AeroTraNet 2 management board meetings from Airbus SAS (Dr. Alessandro Savarese and Dr. Jerome Huber), and from the EU Desk Officer Sergio Mastropierro, is gratefully acknowledged.

## REFERENCES

1. Tam, C. K. W., Pastouchenko, N. N. and Viswanathan, K. Broadband shock-cell noise from dual stream jets, *J. Sound Vib.*, **324** (3), 861–891, (2009).

2. Tam, C. K. W., Seiner, J. M. and Yu, J. C. Proposed relationship between broadband shock associated noise and screech tones, *J. Sound Vib.*, **110** (2), 309–321, (1986).

3. Panda, J. An experimental investigation of screech noise generation, *J. Fluid Mech.*, **378**, 71–96, (1999).

4. Suzuki, T. and Lele, S. K. Shock leakage through an unsteady vortex-laden mixing layer: application to jet screech, *J. Fluid Mech.*, **490**, 139–167, (2003).

5. Camussi, R., Grilliat, J., Caputi-Gennaro, G., Jacob, M. C., et al. Experimental study of a tip leakage flow: wavelet analysis of pressure fluctuations, *J. Fluid Mech.*, **660**, 87–113, (2010).

6. Lele, S. Compact finite difference schemes with spectral-like resolution, *J. Comput. Phys.*, **103**, 16–42, (1992).

7. Fosso-Pouangué, A., Deniau, H., Sicot, F. and Sagaut, P. Curvilinear finite volume schemes using high order compact interpolation, *J. Comput. Phys.*, **229** (13), 5090–5122, jx, (2010).

8. Visbal, M. and Gaitonde, D. On the use of higher-order finite-difference schemes on curvilinear and deforming meshes, *J. Comput. Phys.*, **181**, 155–185, (2002).

9. Bogey, C. and Bailly, C. A family of low dispersive and low dissipative explicit schemes for flow and noise computations, *J. Comput. Phys.*, **194** (1), 194–214, (2004).

10. Roe, P. Approximate Riemann solvers, parameter vectors and difference schemes, *Journal of Computational Physics*, **43** (2), 357–372, (1981).

11. van Leer, B., Thomas, J., Roe, P. and Newsome, R. A comparison of numerical flux formulas for euler and navier-stokes equation, *AIAA 8th Computational Fluid Dynamics Conference*, **87-1104**, 36–41, (1987).

12. Sweby, P. K. High resolution schemes using flux limiters for hyperbolic conservation laws, *SIAM Journal on Numerical Analysis*, **21** (5), 995–1011, (1984).

13. Wilcox, D., *Turbulence modeling for CFD*, Griffin Printing, Glendale, California, USA (2002).

14. Yoshizawa, A. Statistical theory for compressible shear flows with the application of subgrid modelling, *Physics of Fluids*, **29**, 2152–63, (1986).

15. Menter, F. NASA Tech. Mem., Improved two-equation $k-\omega$ turbulence models for aerodynamic flows, (1992).

16. El-Dosoki, M. F. F., *Analytical and CFD Methods Investigating Shroud Blade Tip Leakage*, Ph.D. thesis, University of Leicester, Leicester, UK, (2009).

17. Grottadaurea, M. and Rona, A. Detached eddy simulation of subsonic cylindrical cavity flow, *Science and supercomputing in Europe*, pp. 364–369, (2008).

18. Di Pasquale, D. and Rona, A. Data assessment of two ercoftac transition test cases for cfd validation, *7th International Conference on Heat Transfer, Fluid Mechanics and Thermodynamics, 19-21 July 2010, Antalya, Turkey*, (2010).

19. Pérez Arroyo, C. Simulation of shock cell noise with elsa solver, *UK NFP 2014 Workshop, 2nd April, Manchester, UK*, (2014).

20. Pérez-Arroyo, *Large eddy simulations of a dual stream jet with shock-cells and noise emission analysis*, Ph.D. thesis, Université de Toulouse, Toulouse, France, (2016).

21. Savarese, A., Jordan, P., Girard, S., Royer, A., Fourment, C., Collin, E., Gervais, Y. and Porta, M. Experimental study of shock-cell noise in underexpanded supersonic jets, *AIAA J.*, (2013).

22. Bidadi, S., Pérez Arroyo, C., Puigt, G. and Boussuge, J.-F. A high-order adaptive finite volume methodology for shock-turbulence interaction, *Journal of Computational Physics*, submitted, (2016).